

Multiphoton microscopy with near infrared contrast agents

Siavash Yazdanfar,^{a,*} Chulmin Joo,^a Chun Zhan,^a Mikhail Y. Berezin,^b Walter J. Akers,^b and Samuel Achilefu^b

^aGE Global Research, Applied Optics Laboratory, 1 Research Circle, Niskayuna, New York 12309

^bWashington University, School of Medicine, Department of Radiology, 4525 Scott Avenue, St. Louis, Missouri 63110

Abstract. While multiphoton microscopy (MPM) has been performed with a wide range of excitation wavelengths, fluorescence emission has been limited to the visible spectrum. We introduce a paradigm for MPM of near-infrared (NIR) fluorescent molecular probes via nonlinear excitation at 1550 nm. This all-NIR system expands the range of available MPM fluorophores, virtually eliminates background autofluorescence, and allows for use of fiber-based, turnkey ultrafast lasers developed for telecommunications. © 2010 Society of Photo-Optical Instrumentation Engineers. [DOI: 10.1117/1.3420209]

Keywords: two-photon microscopy; ultrafast fiber lasers; near-infrared imaging.

Paper 10063LR received Feb. 8, 2010; revised manuscript received Apr. 5, 2010; accepted for publication Apr. 6, 2010; published online May 10, 2010.

Multiphoton microscopy (MPM) has become an indispensable optical imaging modality due to its intrinsic three-dimensional localization, low photobleaching and photodamage outside the focal volume, and improved imaging depth.¹ MPM typically uses near-infrared (NIR) excitation at 700 to 1000 nm to generate fluorescence in the visible wavelengths.² Although the excitation wavelength of MPM has been extended^{3–8} beyond 1000 nm, to our knowledge no imaging has been performed with NIR-emitting contrast agents. Conventional (linear) fluorescence imaging has shown that molecular imaging with NIR (>700 nm) agents minimizes the contribution from endogenous fluorescence and increases penetration depth.⁹ Since conventional MPM efficiently images endogenous molecules such as collagen, elastin, and reduced nicotinamide adenine dinucleotide (NADH),¹⁰ the signal from these and other endogenous fluorophores restricts molecular imaging with exogenous contrast agents. This is particularly problematic when target concentrations are low, and strategies to reduce autofluorescence become critical to image contrast. Here, we measure two-photon-induced fluorescence of NIR dyes and demonstrate their use for autofluorescence-free biological imaging.

Heptamethine cyanine dyes were selected as NIR contrast agents because of their biocompatibility and the availability of diverse structures with single photon (1P) absorption and emission between 700 and 850 nm. Cypate, a derivative of

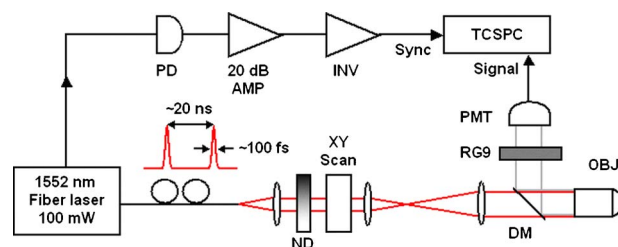


Fig. 1 Schematic diagram of all-NIR multiphoton microscope. PD, photodiode; INV, inverter; ND, neutral density filter; DM, dichroic mirror; OBJ, objective lens; RG9, Schott glass filter; PMT, photomultiplier tube; and TCSPC, time-correlated single photon counting card.

indocyanine green, was prepared as previously reported,¹¹ and 3,3'-diethylthiatricarbocyanine iodide (DTTCI) were purchased from a commercial source (Sigma-Aldrich, Saint Louis, Missouri). These dyes exhibit an absorption/emission peak of 799/817 nm and 771/800 nm, respectively. Fortunately, these absorption maxima of NIR dyes correspond to roughly half the telecommunications spectral window at 1550 nm. As this overlaps with the gain spectrum of erbium, we perform all-NIR MPM using a simple, turnkey erbium-doped fiber laser. A mode-locked femtosecond fiber laser (Mercury 1000, PolarOnyx, Sunnyvale, California) provided 100 mW of excitation light at ~1550 nm through a ~1-m optical fiber (Fig. 1). At the output of the fiber, the pulse duration was nominally 100 fs with a repetition rate of 50 MHz, although positive material dispersion of the optical components in the system leads to pulse broadening and reduces excitation efficiency at the sample. These losses can be recovered if the pulses arriving at the sample are transform-limited by precompensating for material dispersion in the system,¹² for example with a prism pair. In the present scheme, since the laser is designed to provide transform-limited pulses at the output of a 1-m fiber, we reduced the length of the fiber (to ~0.75 m) as a simple, albeit not continuously variable, method of dispersion precompensation.

The laser light was collimated and passed through neutral density filters for controlling the incident power on the sample (between 5 to 20 mW). The beam was then expanded (5×), directed through a dichroic mirror (LP02-980RS, Semrock, Rochester, New York), and focused onto the sample using a 20×, 0.8-NA Plan-Apochromat (Zeiss) objective lens. Two-photon (2P) epifluorescence from the sample was collected through the same objective and directed toward the detector using the dichroic mirror. The detector was a thermoelectrically cooled, red-enhanced photomultiplier tube (PMT) (PMC-100-20, Becker-Hickl, Berlin, Germany). The seed monitor of the laser triggered data acquisition using a time-correlated single photon counting (TCSPC) card (SPC-730, Becker-Hickl). Although the PMT cathode sensitivity appeared to be negligible at the excitation wavelength, residual excitation light was further removed using a 1-mm-thick RG9 Schott glass filter. This filter also served to minimize stray light in the visible wavelength range. Images were acquired by raster scanning the excitation beam with a galvanometric mirror pair (GSI Group, Bedford, Massachusetts), centered near a conjugate plane of the back focal plane of the objective

*Address all correspondence to: Siavash Yazdanfar. Tel: 518-387-4492; Fax: 518-387-7021; E-mail: siavash.yazdanfar@research.ge.com

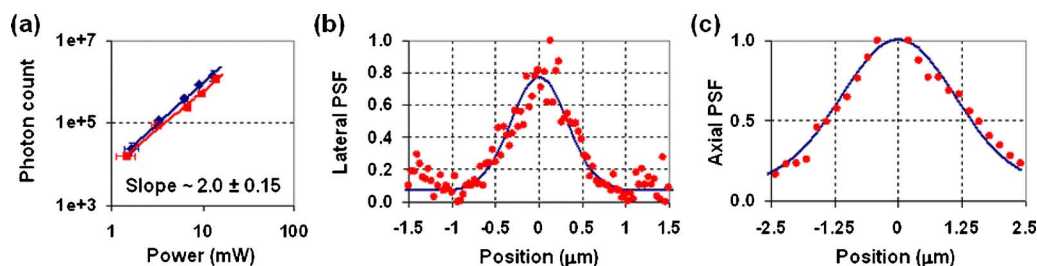


Fig. 2 (a) Quadratic dependence of fluorescence on excitation power indicates 2P process. Error bars in the abscissa are 0.3 mW, determined by the power meter resolution. Error bars in the ordinate are the standard deviation of three measurements. (b) Lateral and (c) axial point spread functions (PSFs).

lens to approximate telecentric scanning and thus a flat field of view (FOV). The pixel integration time varied from 5 to 15 msec, limited by TCSPC. Collected images were analyzed with a single photon counting module (SPCM) and SPCImage software (Becker-Hickl). The total fluorescence photon count scaled quadratically with the average incident power at the sample [a slope of 2.0 ± 0.15 on a log-log plot, Fig. 2(a)], verifying that the measured signals were indeed due to a 2P process.¹ Using 200-nm fluorescently labeled particles embedded in agarose gel, the lateral and axial resolutions [Figs. 2(b) and 2(c)] were measured as ~ 0.77 and $\sim 2.64 \mu\text{m}$, respectively, which agreed to within 5% of the theoretical calculation.¹³ The longer emission wavelengths in this system result in ~ 1.5 to $2\times$ lower resolution than MPM of visible dyes.

Having thus attributed NIR fluorescence to 2P excitation, we explored the feasibility of biological imaging with these dyes. All animal studies were performed in compliance with the Washington University School of Medicine Animal Studies Committee requirements for the humane care and use of laboratory animals in research. Human epithelial carcinoma xenografts were grown in nude mice by injection of A431 cells. Tumor tissue was harvested and snap-frozen. $10\text{-}\mu\text{m}$ cryostat sections were stained with cypate or DTTCl by incubating with $200 \mu\text{L}$ of $1\text{-}\mu\text{M}$ dye in phosphate buffered saline (PBS) for 1 h, and rinsed with PBS three times for 5 min

each. Coverslips were applied and sealed with nail polish. Figure 3 presents all-NIR 2P images (256×256 pixels) of $10\text{-}\mu\text{m}$ -thick sections of human epithelial carcinoma tissues labeled with the NIR dyes, which localized in the cell membranes and stromal tissues but did not stain the nuclei, shown as dark regions. The benefits of all-NIR imaging are observed by imaging unlabelled samples (Fig. 4) using a wide-field upright 1P microscope (Zeiss Axio Imager.Z1, $20\times$ 0.8-NA Plan-Apochromat objective) at $790 \pm 25 \text{ nm}$ for NIR excitation and $450 \pm 50 \text{ nm}$ for visible excitation. A comparison of histograms and images, using the same intensity color scale, indicated a dramatic reduction in NIR autofluorescence. In practice, reducing the background should result in higher contrast imaging, in particular for targeted molecular imaging. Since water absorption is higher at 1550 nm than at conventional MPM excitation wavelengths, the possibility of thermal damage both within and outside the focus needs to be explored. In preliminary imaging with ten samples, no heating effects were observed from repeated imaging. Further studies are needed to examine the potentially deleterious effects of imaging in this spectral band, although previous reports at this excitation wavelength^{4,5} have likewise not reported damage at low power levels. Another potential disadvantage of imaging in this spectral window is the lower quantum efficiency and higher dark noise of detectors in the NIR, which may result in lower contrast imaging.

We have developed an all-NIR MPM instrument for imaging dyes with emission above 700 nm . Imaging of NIR fluo-

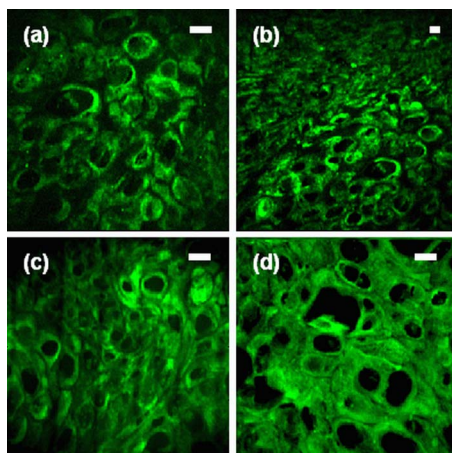


Fig. 3 All-NIR 2P fluorescence microscopy images of A431 human carcinoma tissue sections labeled with NIR dyes (a) and (b) DTTCl and (c) and (d) cypate. Incident power was $<10 \text{ mW}$. The scale bar is $20 \mu\text{m}$. (Color online only.)

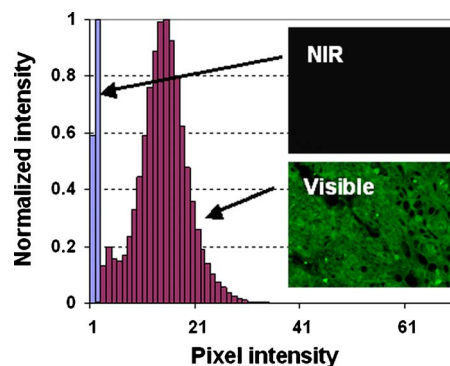


Fig. 4 Dramatically attenuated NIR autofluorescence is exhibited by unlabelled A431 human epithelial cells under NIR and visible 1P excitation. Intensities are shown on the same color scale for comparison. 2P imaging of unlabelled samples similarly yielded blank images. Field of view $\sim 1 \text{ mm}$. (Color online only.)

rophores expands the available spectrum for MPM, minimizes autofluorescence, and may potentially improve penetration depth. This simple and affordable turnkey fiber-based laser system could serve as a platform for characterizing and imaging other NIR fluorophores^{14,15} near 1550 nm. While 2P excitation spectra do not consistently mirror the 1P absorption spectra,² in many cases the 2P excitation peak is at or near twice the wavelength of the 1P peak. Therefore, dyes with 1P peaks near 775 nm, or half the 2P excitation laser in our experiment, are generally expected to demonstrate a high 2P action cross section. The use of tunable lasers would provide flexibility in the choice of NIR fluorescent dyes for all-NIR MPM, improve 2P cross sections, and enhance the resultant fluorescence by exciting the molecules at their maximum 2P absorption wavelengths. In addition, spectroscopic detection using an optical parametric oscillator⁴ can be used to identify the optimal excitation wavelength of the dyes. Alternatively, dyes can be engineered for improved 2P absorption within the NIR spectral range of our current instrument.

NIR emission does not compromise many existing advantages of 2P microscopy, such as multiplexing of fluorophores. Multiplexed detection can be achieved by adapting the system to cover additional spectral ranges, for example, by combining the NIR light source with conventional Ti:sapphire lasers or novel fiber-based or solid state light sources.^{16–18} Frequency doubling of the fiber laser would result in a second excitation wavelength at 775 nm, comparable to conventional MPM, in addition to the fundamental wavelength near 1550 nm. The former can be used to excite visible dyes, and the latter NIR dyes. Multimodal microscopy is feasible on this imaging platform, combining 2P with higher order MPM of visible dyes,⁴ harmonic generation,³ optical coherence microscopy,¹⁰ or autoconfocal microscopy.¹⁹ In conclusion, we have demonstrated 2P microscopy with NIR contrast agents and a fiber laser at 1550 nm. This system widens the spectral window available for molecular imaging with MPM and virtually eliminates autofluorescence. We anticipate that this technology can be rapidly adopted for use in intravital imaging of living tissues that are accessible to endoscopes and catheters.

Acknowledgments

This study was supported by a grant from the National Institutes of Health (R21/R33 CA12353701). We acknowledge S. Bhaumik, A. Sood, and J. DePuy for help in sample preparation, and P. Codella for performing linear spectroscopy.

References

1. W. Denk, J. H. Strickler, and W. W. Webb, "Two-photon laser scanning fluorescence microscopy," *Science* **248**, 73–76 (1990).
2. C. Xu and W. W. Webb, "Measurement of two-photon excitation cross sections of molecular fluorophores with data from 690 to 1050 nm," *J. Opt. Soc. Am. B* **13**, 481–491 (1996).
3. S. W. Chu, I. H. Chen, T. M. Liu, P. C. Chen, C. K. Sun, and B. L. Lin, "Multimodal nonlinear spectral microscopy based on a femto-second Cr:forsterite laser," *Opt. Lett.* **26**, 1909–1911 (2001).
4. G. McConnell, "Nonlinear optical microscopy at wavelengths exceeding 1.4 μm using a synchronously pumped femtosecond-pulsed optical parametric oscillator," *Phys. Med. Biol.* **52**, 717–724 (2007).
5. D. Trüttelein, F. Adler, K. Moutzouris, A. Jeromin, A. Leitenstorfer, and E. Ferrando-May, "Highly versatile confocal microscopy system based on a tunable femtosecond Er: fiber source," *J. Biophoton.* **1**, 53–61 (2008).
6. M. Balu, T. Baldacchini, J. Carter, T. B. Krasieva, R. Zadoyan, and B. J. Tromberg, "Effect of excitation wavelength on penetration depth in nonlinear optical microscopy of turbid media," *J. Biomed. Opt.* **14**, 010508 (2009).
7. V. Andresen, S. Alexander, W. H. Heupel, M. Hirschberg, R. M. Hoffman, and P. Friedl, "Infrared multiphoton microscopy: subcellular-resolved deep tissue imaging," *Curr. Opin. Biotechnol.* **20**, 54–62 (2009).
8. D. Kobat, M. E. Durst, N. Nishimura, A. W. Wong, C. B. Schaffer, and C. Xu, "Deep tissue multiphoton microscopy using longer wavelength excitation," *Opt. Express* **17**, 13354–13364 (2009).
9. E. M. Sevick-Muraca and J. C. Rasmussen, "Molecular imaging with optics: primer and case for near-infrared fluorescence techniques in personalized medicine," *J. Biomed. Opt.* **13**, 041303 (2008).
10. S. Yazdanfar, Y. Y. Chen, P. T. C. So, and L. H. Laiho, "Multifunctional imaging of endogenous contrast by simultaneous nonlinear and optical coherence microscopy of thick tissues," *Microsc. Res. Tech.* **70**, 628–633 (2007).
11. S. Achilefu, R. B. Dorshow, J. E. Bugaj, and R. Rajagopalan, "Novel receptor-targeted fluorescent contrast agents for in vivo tumor imaging," *Invest. Radiol.* **35**, 479–485 (2000).
12. D. K. Kim, H. J. Choi, S. Yazdanfar, and P. T. C. So, "Ultrafast optical pulse delivery with fibers for nonlinear microscopy," *Microsc. Res. Tech.* **71**, 887–896 (2008).
13. M. Gu, "Image formation in multiphoton fluorescence microscopy," in *Handbook of Biomedical Nonlinear Optical Microscopy*, B. R. Masters and P. T. C. So, Eds., pp. 266–282, Oxford University Press, New York (2008).
14. Y. P. Ye, S. Bloch, B. G. Xu, and S. Achilefu, "Design, synthesis, and evaluation of near infrared fluorescent multimeric RGD peptides for targeting tumors," *J. Med. Chem.* **49**, 2268–2275 (2006).
15. M. Y. Berezin, H. Lee, W. Akers, and S. Achilefu, "Near infrared dyes as lifetime solvatochromic probes for micropolarity measurements of biological systems," *Biophys. J.* **93**, 2892–2899 (2007).
16. J. R. Unruh, E. S. Price, R. G. Molla, L. Stehno-Bittel, C. K. Johnson, and R. Q. Hui, "Two-photon microscopy with wavelength switchable fiber laser excitation," *Opt. Express* **14**, 9825–9831 (2006).
17. S. Sakadžić, U. Demirbas, T. R. Mempel, A. Moore, S. Ruvinskaya, D. A. Boas, A. Sennaroglu, F. X. Kartner, and J. G. Fujimoto, "Multiphoton microscopy with a low-cost and highly efficient Cr:LiCAF laser," *Opt. Express* **16**, 20848–20863 (2008).
18. S. Tang, J. Liu, T. B. Krasieva, Z. P. Chen, and B. J. Tromberg, "Developing compact multiphoton systems using femtosecond fiber lasers," *J. Biomed. Opt.* **14**, 030508 (2009).
19. C. Joo, C. Zhan, Q. Li, and S. Yazdanfar, "Autoconfocal transmission microscopy based on two-photon induced photocurrent of Si photodiodes," *Opt. Lett.* **35**, 67–69 (2010).